Inorg. Chem. **1998,** *37,* 4573−4577

Synthesis and Electrochemistry of Tin(IV) Octaethylcorroles, (OEC)Sn(C_6H_5) and (OEC)SnCl

Karl M. Kadish,*,[†] Stefan Will,[‡] Victor A. Adamian,[†] Burkhard Walther,[‡] Christoph Erben,[‡] Zhongping Ou,[†] Ning Guo,[†] and Emanuel Vogel*,[‡]

Department of Chemistry, University of Houston, Houston, Texas 77204-5641,
and Institut für Organische Chemie, Universität zu Köln, Greinstrasse 4, 50939 Köln, Germany

Received March 12, 1998

Two Sn(IV) corroles were synthesized and electrochemically examined. The investigated compounds are represented as (OEC)Sn(C_6H_5) and (OEC)SnCl, where OEC = trianion of 2,3,7,8,12,13,17,18-octaethylcorrole. (OEC)Sn(C_6H_5) represents the first example of a σ-bonded metallocorrole which does not undergo a metal-centered electrode reaction. Both compounds undergo three reversible one-electron oxidations, all of which occur at the conjugated macrocycle. The reduction of (OEC)SnCl involves an overall two electrons, with the product being spectroscopically identified as a Sn(II) corrole after bulk electrolysis of the starting compound. (OEC)Sn(C_6H_5) is reversibly reduced by a single electron to give a Sn(IV) corrole π-anion radical. The electrochemically measured HOMO−LUMO gap (defined as the absolute potential difference between the first-ring centered reduction and first ring-centered oxidation) is equal to 2.25 V in benzonitrile, a value which closely approximates what is observed for porphyrins containing octaethylporphyrin (OEP) or tetraphenylporphyrin (TPP) macrocycles. An X-ray crystallographic analysis for the molecular structure of (OEC)Sn(C_6H_5) is also presented: monoclinic, $P2_1/n$, with $a = 13.235(4)$ Å, $b = 14.502(4)$ Å, $c = 18.387(5)$ Å, $\beta = 95.45(2)°$, $Z = 4$, $R = 0.0619$.

Introduction

The corroles are structurally close to the porphyrins, as shown in Chart 1 for the free base octaethylcorrole, (OEC)H_3, and octaethylporphyrin, (OEP)H_2, derivatives, but differ in the charge of the deprotonated macrocycle, which is −3 for the corrole and −2 for the porphyrin.[1] As a consequence, the corrole macrocycle is able to stabilize metal ions in higher oxidation states than the corresponding porphyrin macrocycle.[1−7]

The metallocorroles also possess different electrochemical properties compared to the corresponding metalloporphyrins.[2−7] In particular, the metallocorroles are easier to oxidize and show more oxidations than metalloporphyrins[8] containing the same central metal ion. Three[2−5] or four[6] oxidations have been observed for cobalt and iron corroles, some of which involve the central metal ion and others the conjugated macrocycle. However, an evaluation as to the exact site of electrooxidation in a given electrode reaction was not obvious because of extensive interactions which exist[2,3] between the orbitals of the macrocycle and those of the electroactive transition metal ion.

Chart 1

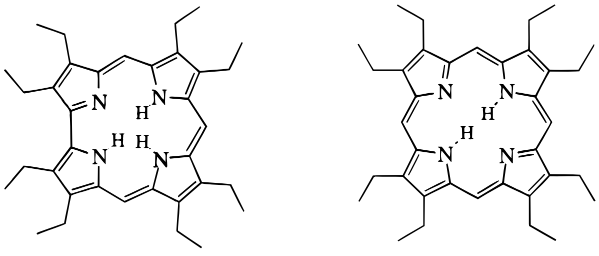

(OEC)H_3 **(OEP)H_2**

We have now synthesized two Sn(IV) corroles which cannot undergo oxidation at the central metal and, therefore, provide model complexes where all of the oxidations must occur at the conjugated π ring system of the corrole macrocycle. The investigated compounds are represented as (OEC)Sn(C_6H_5) and (OEC)SnCl, where OEC = trianion of 2,3,7,8,12,13,17,18-octaethylcorrole. (OEC)Sn(C_6H_5), which was structurally characterized, represents the third example of a metallocorrole containing a phenyl σ-bonded axial ligand, but unlike (OEC)-Fe(C_6H_5)[2] and (OEC)Co(C_6H_5),[3] it is the only such complex which does not undergo a metal-centered electrode reaction. Both corroles were also examined as to their electrochemistry in dichloromethane and benzonitrile, and a comparison of the data is made with related tin(IV) porphyrins containing halide[9−14] or σ-bonded[15,18] axial ligands.

[†] University of Houston.

[‡] Universität zu Köln.

(1) (a) Johnson, A. W. *Pure Appl. Chem.* **1970**, *23*, 375. (b) Genokhova, N. S.; Melent'eva, T. A.; Berezovskii, V. M. *Russ. Chem. Rev.* **1980**, *49*, 1056. (c) Melent'eva, T. A. *Russ. Chem. Rev.* **1983**, *52*, 641. (d) Licoccia, S.; Paolesse, R. *Struct. Bonding* **1995**, *84*, 71.

(2) (a) Vogel, E.; Will, S.; Schulze Tilling, A.; Neumann, L.; Lex, J.; Bill, E.; Trautwein, A. X.; Wieghardt, K. *Angew. Chem.* **1994**, *106*, 771; *Angew. Chem., Int. Ed. Engl.* **1994**, *33*, 731. (b) Van Caemelbecke, E.; Will, S.; Autret, M.; Adamian, V. A.; Lex, J.; Gisselbrecht, J.-P.; Gross, M.; Vogel, E.; Kadish, K. M. *Inorg. Chem.* **1996**, *35*, 184.

(3) Will, S.; Lex, J.; Vogel, E.; Adamian, V. A.; Van Caemelbecke, E.; Kadish, K. M. *Inorg. Chem.* **1996**, *35*, 5577.

(4) Kadish, K. M.; Koh, W.; Tagliatesta, P.; Sazou, D.; Paolesse, R.; Licoccia, S.; Boschi, T. *Inorg. Chem.* **1992**, *31*, 2305.

(5) Autret, M.; Will, S.; Van Caemelbecke, E.; Lex, J.; Gisselbrecht, J.-P.; Gross, M.; Vogel, E.; Kadish, K. M. *J. Am. Chem. Soc.* **1994**, *116*, 9141.

(6) Adamian, V. A.; D'Souza, F.; Licoccia, S.; Di Vona, M. L.; Tassoni, E.; Paolesse, R.; Boschi, T.; Kadish, K. M. *Inorg. Chem.* **1995**, *34*, 532.

(7) Matsuda, Y.; Yamada, S.; Murakami, Y. *Inorg. Chem.* **1981**, *20*, 2239.

(8) Kadish, K. M. *Prog. Inorg. Chem.* **1986**, *34*, 435.

Table 1. Crystallographic Data for (OEC)Sn(C_6H_5)

empirical formula	$C_{41}H_{48}N_4Sn$
fw	715.52
cryst syst	monoclinic
space group	$P2_1/n$
Z	4
a, Å	13.235(4)
b, Å	14.502(4)
c, Å	18.387(5)
β, deg	95.45(2)
V, Å^3	3513(2)
T, K	293(2)
wavelength, Mo Kα, Å	0.710 69
ρ_{calcd}, g cm^{-3}	1.353
μ_{Mo}, mm^{-1}	0.762
data: unique/obsd	5061/4925
no. of params	609
R1 (F_o, $I > 2(I)$)[a]	0.0619
wR2 (F_o^2)[b]	0.1394

[a] $R1 = [\sum||F_o| - |F_c||]/[\sum|F_o|]$. [b] $wR2 = \{[\sum w(F_o^2 - F_c^2)^2]/[\sum w(F_o^2)^2]\}^{1/2}$.

Experimental Section

Instrumentation. ^{1}H NMR spectra were recorded on a Bruker AP 300 NMR spectrometer at 300 MHz. The solvent signal at $\delta = 7.24$ ppm was used as a standard. Cyclic voltammetry was carried out with an EG&G Model 173 potentiostat or an IBM Model EC 225 voltammetric analyzer. A three-electrode system was used and consisted of a glassy carbon or platinum disk working electrode, a platinum wire counter electrode, and a saturated calomel electrode (SCE) as the reference electrode. Thin layer and bulk coulometry were used for measuring the number of electrons transferred. Ferrocene was used as an internal standard. All potentials are referenced to the SCE. UV−visible spectroelectrochemical experiments were carried out with a Hewlett-Packard Model 8452A diode array spectrophotometer. UV−visible spectra were recorded on a Perkin-Elmer Lambda 7 spectrophotometer, while IR measurements were performed with a Perkin-Elmer IR 283 or a Perkin-Elmer Series 1600 spectrometer. Mass spectra were obtained using a Finnigan MAT 212. ESR spectra were recorded on an IBM ER 100D or on a Bruker ESP 380E spectrometer. The g values were measured with respect to diphenylpicrylhydrazyl ($g = 2.0036 \pm 0.0003$). Elemental analyses were provided by BAYER AG (Leverkusen, Germany).

X-ray Structural Determination of (OEC)Sn(C_6H_5). X-ray data were collected on an Enraf-Nonius CAD4 diffractometer using monochromated Mo Kα radiation. Experimental conditions are given in Table 1. Cell parameters were determined by least-squares refinement of 25 arbitrary reflections. The intensities of two standard reflections were checked every 2 h. The structures were solved by direct methods and refined against F_o^2 for all observed reflections (non-hydrogen atoms with anisotropic, hydrogen atoms with isotropic temperature factors) using the SHELXL-93 program package.[19] The final model shows no peaks and holes larger than 2.180 and −1.085 e/Å^3, respectively.

Chemicals. Benzonitrile (PhCN) was purchased from Aldrich Chemical Co. and distilled over P_2O_5 under vacuum prior to use. Absolute dichloromethane (CH_2Cl_2) and dimethylformamide (DMF) were purchased from Aldrich Chemical Co. and used without further purification. $CDCl_3$, used for NMR measurements, was obtained from Aldrich Chemical Co. and used as received. Tetra-*n*-butylammonium perchlorate (TBAP) was purchased from Sigma Chemical Co., recrystallized from ethyl alcohol, and dried under vacuum at 40 °C for at least 1 week prior to use.

(OEP)SnCl$_2$. (2,3,7,8,12,13,17,18-Octaethylporphyrinato)tin(IV)-chloride was synthesized at the University of Dijon according to literature procedures.[14]

(OEC)SnCl. A 20 mL DMF solution containing 523 mg (1 mmol) of free base octaethylcorrole and 380 mg (2 mmol) of tin(II) chloride was refluxed for 1 h and then stored in the refrigerator for 6 h, during which time a red precipitate was formed. This precipitate was collected and washed with methanol. The crude product was then purified by being passed through a short column of silica gel, dichloromethane being used as eluent. After crystallization from hexane, the title compound, (OEC)SnCl, was obtained as a red powder (yield: 430 mg, 64%). Mp: 227−229 °C. ^{1}H NMR (300 MHz, $CDCl_3$): $\delta = 9.80$ (singlet, 2H, H-5,15), 9.68 (singlet, 1H, H-10), 4.15 (multiplet, 4H, H-2a,18a), 4.08 (multiplet, 4H, H-7a,13a), 4.07 (multiplet, 4H, H-8a,-12a), 4.04 (multiplet, 4H, H-3a,17a), 1.91 (triplet, 6H, H-7b,13b), 1.88 (triplet, 6H, H-3b,17b), 1.86 (triplet, 12H, H-2b,8b,12b,18b). ^{13}C NMR (75.5 MHz, $CDCl_3$): $\delta = 140.74$ (C-9,11), 140.24 (C-7,13), 140.13 (C-3,17), 137.89 (C-4,16), 136.56 (C-8,13), 135.55 (C-6,14), 132.61 (C-2,18), 131.58 (C-1,19), 94.42 (C-5,15), 89.04 (C-10), 20.89 (C-2a,-18a), 20.03 (C-7a,13a), 19.89 (C-3a,17a), 19.65 (C-8a,12a), 18.66 (C-2b,18b), 18.58 (C-7b,13b), 18.04 (C-3b,17b), 17.85 (C-8b,12b). IR (CsI): $\nu = 2964$, 2930, 2869, 1474, 1462, 1447, 1374, 1316, 1274, 1194, 1160, 1056, 1025, 1011, 995, 959, 882, 825, 815, 755 cm^{-1}. UV−vis (CH_2Cl_2): λ_{max} (nm) (ϵ, mol^{-1} L cm^{-1}) = 280 (15 400), 318 (14 900), 387 (62 500), 409 (367 000), 532 (14 400), 566 (48 500).

(OEC)Sn(C_6H_5). (Phenyl)(2,3,7,8,12,13,17,18-octaethylcorrolato)-tin(IV) was obtained by either of the two following methods:

Method A. Octaethylcorrole (262 mg; 0.5 mmol) and 1.44 g (5 mmol) of diphenyltin oxide in 10 mL of dry DMF were heated to 140 °C under an argon atmosphere for 5 h. After cooling to room temperature, 100 mL of toluene was added. The mixture was filtered and washed with 0.5 M hydrochloric acid (100 mL), water (100 mL), and a sodium hydrogen carbonate solution (100 mL). After drying over sodium sulfate, the solution was evaporated to dryness. Chromatography on silica gel using hexane/toluene (2/1) as eluent gave a purple eluate, from which the σ-phenyl complex was crystallized from hexane as purple rhombuses (yield 190 mg, 53%).

Method B. To a solution of 337 mg (0.5 mmol) of (OEC)SnCl in dichloromethane was added 2 mmol of phenylmagnesium bromide in diethyl ether, and the solution was stirred for 5 min. Aqueous ammonium chloride was added, after which the organic layer was extracted with water and then evaporated to dryness. The residue was passed through a column of silica gel using dichloromethane/hexane (1/1) as eluent. The purple band contained the title compound, which was obtained after crystallization from hexane as purple rhombuses (yield 301 mg, 84%). Mp: 254−256 °C. ^{1}H NMR (300 MHz, $CDCl_3$): $\delta = 9.71$ (singlet, 2H, H-5,15), 9.53 (singlet, 1H, H-10), 6.25 (triplet, 1H, phenyl, *p*-H), 5.94 (multiplet, 2H, phenyl, *m*-H), 4.21−4.09 (multiplet, 4H, H-2a,18a), 4.20−4.01 (multiplet, 4H, H-3a,17a), 4.12−3.97 (multiplet, 4H, H-7a,13a), 4.17−3.94 (multiplet, 4H, H-8a,-12a), 3.44 (triplet, 2H, phenyl, *o*-H), 1.90 (triplet, 6H, H-3b,17b), 1.87 (triplet, 6H, H-7b,13b), 1.85 (triplet, 6H, H-2b,18b), 1.83 (triplet, 6H, H-8b,12b). ^{13}C NMR (75.5 MHz, $CDCl_3$): $\delta = 141.64$ (C-9,11), 139.31 (C-7,13), 138.95 (C-3,17), 138.35 (C-4,16), 136.41 (C-6,14), 135.69 (C-8,12), 132.98 (C-1,19), 131.88 (phenyl, C_{ipso}), 131.73 (phenyl, *o*-C), 131.33 (C-2,18), 128.37 (phenyl, *p*-C), 126.66 (phenyl, *m*-C), 93.83 (C-5,15), 87.71 (C-10), 20.83 (C-2a,18a), 20.00 (C-3a,17a), 19.88 (C-7a,13a), 19.65 (C-8a,12a), 18.78 (C-2b,18b), 18.67 (C-3b,17b), 18.16 (C-7b,13b), 17.95 (C-8b,12b). MS (EI, 70 eV): *m/z* (%) 716 (100) $[M]^+$, 701 (8) $[M - CH_3^\bullet]^+$, 639 (5) $[M - C_6H_5^\bullet]^+$, 358 (20) $[M]^{2+}$. IR (CsI): $\nu = 3062$, 2965, 2931, 2869, 1464, 1450, 1431, 1372, 1275,

---

(9) Cloutour, C.; Debaig-Valade, C.; Pommier, J.-C. *J. Organomet. Chem.* **1981**, *220*, 21.

(10) Felton, R. H.; Linschitz, H. *J. Am. Chem. Soc.* **1966**, *88*, 1113.

(11) Fuhrhop, J.-H.; Lumbantobing, T. *Tetrahedron Lett.* **1970**, 2815.

(12) Szulbinski, W.; Zak, J.; Strojek, J. W. *J. Electroanal. Chem.* **1987**, *226*, 157.

(13) Fuhrhop, J.-H.; Kadish, K. M.; Davis, D. G. *J. Am. Chem. Soc.* **1973**, *95*, 5140.

(14) Kadish, K. M.; Swistak, C.; Boisselier-Cocolios, B.; Barbe, J.-M.; Guilard, R. *Inorg. Chem.* **1986**, *25*, 4336. (b) Kadish, K. M.; Xu, Q. Y. Y.; Maiya, G. B.; Barbe, J.-M.; Guilard, R. *J. Chem. Soc., Dalton Trans.* **1989**, 1531.

(15) Kadish, K. M.; Dubois, D.; Koeller, S.; Barbe, J.-M.; Guilard, R. *Inorg. Chem.* **1992**, *31*, 3292.

(16) Paolesse, R.; Licoccia, S.; Boschi, T. *Inorg. Chim. Acta* **1990**, *178*, 9.

(17) Hoard, J. L. In *Porphyrins and Metalloporphyrins*; Smith, K. M., Ed.; Elsevier: Amsterdam, 1975; p 328.

(18) Dawson, D. Y.; Sangalang, J. C.; Arnold, J. *J. Am. Chem. Soc.* **1996**, *118*, 6082.

(19) Sheldrick, G. M. *SHELXL-93: Program for the refinement of crystal structures*; University of Göttingen: Göttingen, Germany, 1993.

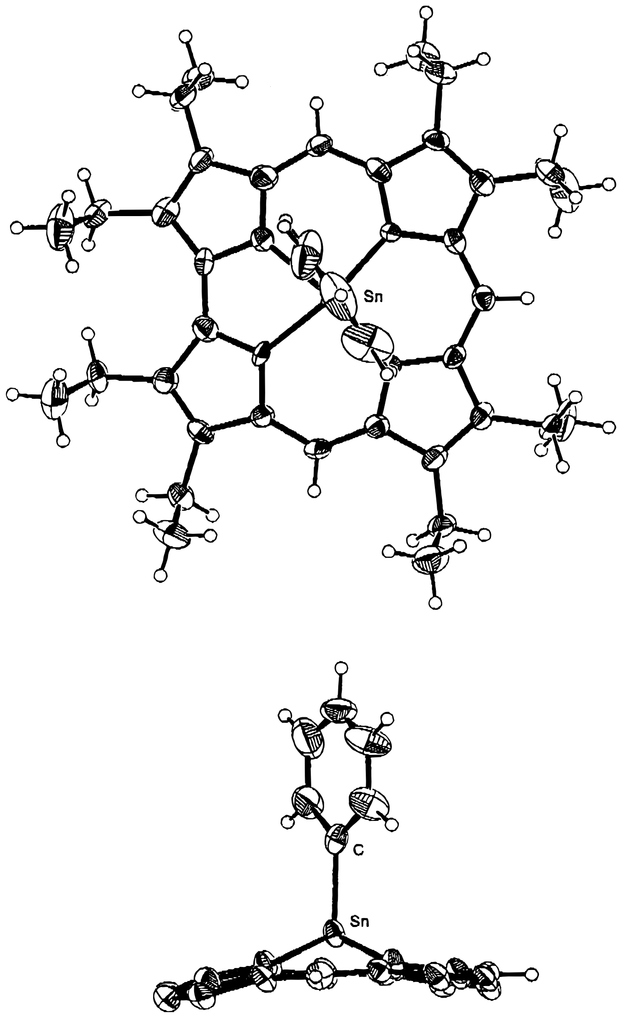

Figure 1. ORTEP diagram of (OEC)Sn(C_6H_5).

1195, 1159, 1056, 1022, 1013, 969, 882, 804, 757, 726, 695 cm^{-1}. UV−vis (CH_2Cl_2): λ_{max}(nm) (ϵ, mol^{-1} L cm^{-1}) = 284 (16 800), 393 (54 700), 415 (327 000), 503 (4100) sh, 540 (11 400), 571 (42 300). Elemental anal. Calcd for $C_{41}H_{48}N_4Sn$: C, 68.82 H, 6.76 N, 7.83. Found: C, 68.80 H, 7.08 N, 7.66.

Results and Discussion

Synthesis. Treatment of the free base corrole with tin(II) chloride in a high-boiling solvent such as DMF or PhCN yielded the tin(IV) complex, (OEC)SnCl, according to a procedure previously reported by Paolesse et al.[16] for the octamethylcorrole derivatives, (OMC)SnCl and (OMC)Sn(CH_3COO). A reaction of the free base corrole, (OEC)H_3, with diphenyltin oxide or a reaction of (OEC)SnCl with phenylmagnesium bromide leads to the same σ-phenyl complex, (OEC)Sn(C_6H_5).

The ^1H NMR spectrum of (OEC)Sn(C_6H_5) confirms the aromaticity of the compound. Resonances of the *meso* protons are located at $\delta = 9.71$ and 9.53 ppm while those of the phenyl protons are detected in the high-field region at 3.44, 5.94, and 6.25 ppm. Characteristic signals due to ^{117}Sn and ^{119}Sn (each $I = {}^1/_2$) coupling are observed for signals of the *ortho* and *meta* protons.

Structural Characterization of (OEC)Sn(C_6H_5). Crystallization of (OEC)Sn(C_6H_5) from hot hexane yielded red prisms suitable for an X-ray structure analysis. The molecular structure of (OEC)Sn(C_6H_5) is given in Figure 1, and experimental data, bond lengths, and angles are presented in Tables 1, 2, and 3, respectively.

Table 2. Bond Lengths (Å) for (OEC)Sn(C_6H_5)

Sn−N(3)	2.062(6)	C(7)−C(8)	1.363(10)
Sn−N(4)	2.065(5)	C(8)−C(9)	1.422(10)
Sn−N(2)	2.069(6)	C(9)−C(10)	1.408(10)
Sn−N(1)	2.072(6)	C(10)−C(11)	1.387(10)
Sn−C(36)	2.105(7)	C(11)−C(12)	1.437(10)
N(1)−C(4)	1.352(9)	C(12)−C(13)	1.362(10)
N(1)−C(1)	1.363(9)	C(13)−C(14)	1.429(10)
N(2)−C(9)	1.377(9)	C(14)−C(15)	1.399(10)
N(2)−C(6)	1.399(9)	C(15)−C(16)	1.386(11)
N(3)−C(14)	1.379(9)	C(16)−C(17)	1.431(10)
N(3)−C(11)	1.386(9)	C(17)−C(18)	1.389(11)
N(4)−C(16)	1.358(9)	C(18)−C(19)	1.439(10)
N(4)−C(19)	1.375(9)	C(20)−C(21)	1.50(2)
C(1)−C(2)	1.434(10)	C(36)−C(37)	1.362(12)
C(1)−C(19)	1.442(10)	C(36)−C(41)	1.379(13)
C(2)−C(3)	1.387(10)	C(37)−C(38)	1.38(2)
C(3)−C(4)	1.430(10)	C(38)−C(39)	1.36(2)
C(4)−C(5)	1.412(10)	C(39)−C(40)	1.37(2)
C(5)−C(6)	1.382(11)	C(40)−C(41)	1.385(14)
C(6)−C(7)	1.425(10)		

Table 3. Bond Angles (deg) for (OEC)Sn(C_6H_5)

N(3)−Sn−N(4)	84.7(2)	N(2)−C(6)−C(7)	107.0(7)
N(3)−Sn−N(2)	88.3(2)	C(8)−C(7)−C(6)	108.6(6)
N(4)−Sn−N(2)	136.8(2)	C(7)−C(8)−C(9)	107.8(6)
N(3)−Sn−N(1)	140.0(2)	N(2)−C(9)−C(10)	123.6(6)
N(4)−Sn−N(1)	74.3(2)	N(2)−C(9)−C(8)	108.3(6)
N(2)−Sn−N(1)	84.6(2)	C(10)−C(9)−C(8)	128.0(7)
N(3)−Sn−C(36)	108.2(3)	C(11)−C(10)−C(9)	127.7(7)
N(4)−Sn−C(36)	112.5(2)	N(3)−C(11)−C(10)	123.9(6)
N(2)−Sn−C(36)	110.2(2)	N(3)−C(11)−C(12)	106.7(6)
N(1)−Sn−C(36)	111.2(3)	C(10)−C(11)−C(12)	129.2(7)
C(4)−N(1)−C(1)	111.7(6)	C(13)−C(12)−C(11)	108.3(6)
C(4)−N(1)−Sn	129.6(5)	C(12)−C(13)−C(14)	108.1(6)
C(1)−N(1)−Sn	118.7(5)	N(3)−C(14)−C(15)	123.9(7)
C(9)−N(2)−C(6)	108.3(6)	N(3)−C(14)−C(13)	107.3(6)
C(9)−N(2)−Sn	124.2(4)	C(15)−C(14)−C(13)	128.5(7)
C(6)−N(2)−Sn	125.8(5)	C(16)−C(15)−C(14)	127.1(7)
C(14)−N(3)−C(11)	109.5(6)	N(4)−C(16)−C(15)	120.6(7)
C(14)−N(3)−Sn	125.4(5)	N(4)−C(16)−C(17)	107.6(6)
C(11)−N(3)−Sn	123.6(4)	C(15)−C(16)−C(17)	131.5(7)
C(16)−N(4)−C(19)	110.2(6)	C(18)−C(17)−C(16)	107.8(6)
C(16)−N(4)−Sn	130.5(5)	C(17)−C(18)−C(19)	106.7(6)
C(19)−N(4)−Sn	119.3(5)	N(4)−C(19)−C(18)	107.5(6)
N(1)−C(1)−C(2)	106.2(6)	N(4)−C(19)−C(1)	112.2(6)
N(1)−C(1)−C(19)	113.2(6)	C(18)−C(19)−C(1)	140.2(7)
C(2)−C(1)−C(19)	140.0(7)	C(37)−C(36)−C(41)	118.0(8)
C(3)−C(2)−C(1)	107.7(6)	C(37)−C(36)−Sn	121.7(6)
C(2)−C(3)−C(4)	107.2(6)	C(41)−C(36)−Sn	120.2(6)
N(1)−C(4)−C(5)	121.1(7)	C(36)−C(37)−C(38)	121.7(12)
N(1)−C(4)−C(3)	107.1(6)	C(39)−C(38)−C(37)	119.3(13)
C(5)−C(4)−C(3)	131.3(7)	C(40)−C(39)−C(38)	120.9(10)
C(6)−C(5)−C(4)	127.0(7)	C(39)−C(40)−C(41)	118.9(12)
C(5)−C(6)−N(2)	123.5(7)	C(40)−C(41)−C(36)	121.0(12)
C(5)−C(6)−C(7)	129.3(7)		

(OEC)Sn(C_6H_5) contains a five-coordinate tin atom placed 0.722(3) Å above the average plane of the four nitrogen atoms. Due to the out-of-plane arrangement of the metal center, the macrocyclic ligand adopts a domed conformation with the pyrrole rings inclined up to 15° with respect to the average plane of the core atoms. Thus, a maximum distance of 0.322 Å of a C or N atom with respect to the average plane defined by the 23 core atoms is observed.

The Sn−N bonds of (OEC)Sn(C_6H_5) are in the range 2.062−2.072 Å and are shorter than similar bonds in the corresponding tin porphyrins, (OEP)Sn$(Cl)_2$ (2.082 Å)[17] and (TPP)Sn$(C_6H_5)_2$ (2.134 Å).[18] The Sn−C bond length in (OEC)Sn(C_6H_5) is 2.105 Å, which is shorter than the Sn−C bonds in (TPP)Sn$(C_6H_5)_2$ (2.158 Å in average)[18] or $(C_6H_5)_3$Sn(OAc) (2.120−2.138 Å).[20] These structural features distinguish the tin compound from σ-bonded metallocorroles with iron[2] and cobalt[3] metal centers

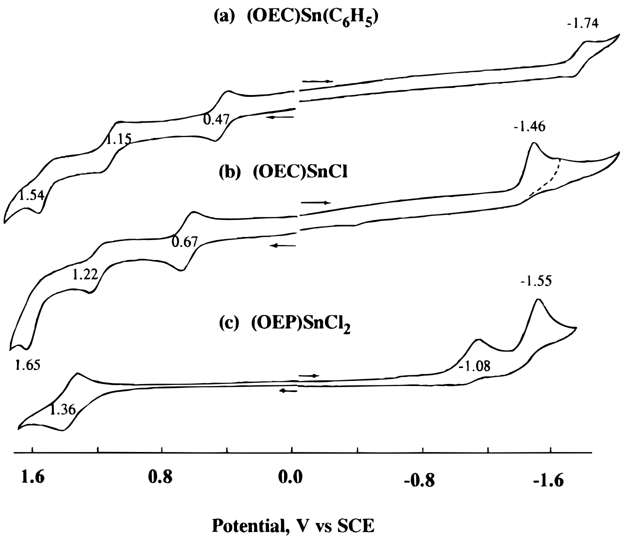

Figure 2. Cyclic voltammograms of (a) $(OEC)Sn(C_6H_5)$, (b) (OEC)SnCl, and (c) $(OEP)SnCl_2$ in CH_2Cl_2 containing 0.1 M TBAP. Scan rate = 0.1 V/s.

Table 4. Half-Wave Potentials (V vs SCE) in CH_2Cl_2 and PhCN Containing 0.1 M TBAP

		oxidation			reduction		
compd	solvent	third	second	first	first	second	$\Delta E_{1/2}$[a]
$(OEC)Sn(C_6H_5)$	CH_2Cl_2	1.54	1.15	0.47	−1.74		2.21
	PhCN		1.12	0.52	−1.73		2.25
(OEC)SnCl	CH_2Cl_2	1.65[b,c]	1.22	0.67	−1.46[d]		2.13[e]
	PhCN	1.69[b]	1.32[b]	0.76	−1.41[d]		2.17[e]
$(OEP)SnCl_2$	CH_2Cl_2			1.36	−1.08	−1.55[d]	2.44
	PhCN			1.35	−1.02	−1.48[d]	2.37

[a] $\Delta E_{1/2}$ = potential difference between the first oxidation and the first reduction. [b] Anodic peak potential, E_{pa}, at scan rate = 0.1 V/s. [c] Reversible $E_{1/2}$ of 1.55 V is measured at −60 °C. [d] Cathodic peak potential, E_{pc}, at scan rate = 0.1 V/s. [e] Based on E_{pc} of reduction.

which exhibit much smaller metal−N_4 distances and a virtually planar macrocyclic ligand.

Electroreduction. Cyclic voltammograms illustrating the oxidation and reduction of $(OEC)Sn(C_6H_5)$, (OEC)SnCl, and $(OEP)SnCl_2$ in CH_2Cl_2 containing 0.1 M TBAP are shown in Figure 2 while the half-wave and peak potentials in CH_2Cl_2 and PhCN are given in Table 4. $(OEC)Sn(C_6H_5)$ undergoes a single reversible one-electron reduction at $E_{1/2} = -1.74$ V in CH_2Cl_2 containing 0.1 M TBAP (see Figure 2). (OEC)SnCl is reduced at $E_{pc} = -1.46$ V for a scan rate of 0.1 V/s, and this process is irreversible at all temperatures between −60 and +25 °C and at all scan rates between 0.025 and 2.5 V/s. The electroreductions of (OEC)SnCl and $(OEC)Sn(C_6H_5)$ differ from that of $(OEP)SnCl_2$ in that the corroles undergo only a single electroreduction process, in contrast to tin(IV) porphyrin, which undergoes two one-electron reductions (see Figure 2 and Table 4).

Controlled-potential reduction of $(OEC)Sn(C_6H_5)$, (OEC)-SnCl, and $(OEP)SnCl_2$ leads to the UV−visible spectral changes shown in Figure 4. The thin-layer spectra of singly reduced $(OEC)Sn(C_6H_5)$ and $(OEP)SnCl_2$ are similar to each other and resemble spectra obtained after the first ring-centered reduction of previously investigated tin(IV) porphyrins.[14] This suggests that the addition of one electron to $(OEC)Sn(C_6H_5)$ also results in formation of a tin(IV) π-anion radical, i.e., $(OEC^{-\bullet})Sn(C_6H_5)$.

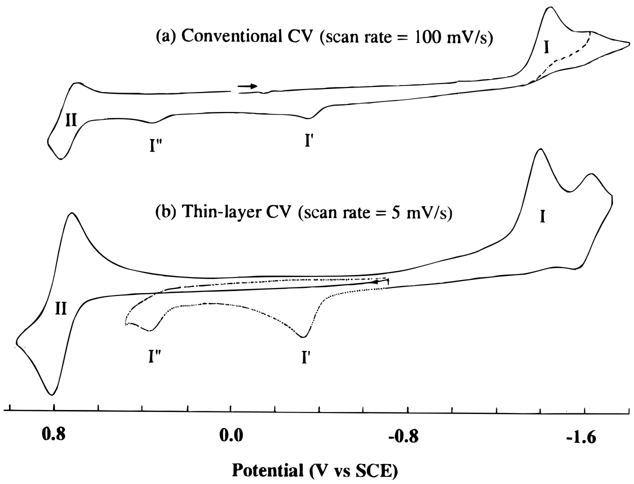

Figure 3. (a) Conventional cyclic voltammogram and (b) thin-layer cyclic voltammogram of (OEC)SnCl in PhCN containing 0.2 M TBAP on initial scan (—) and second scan (- - -).

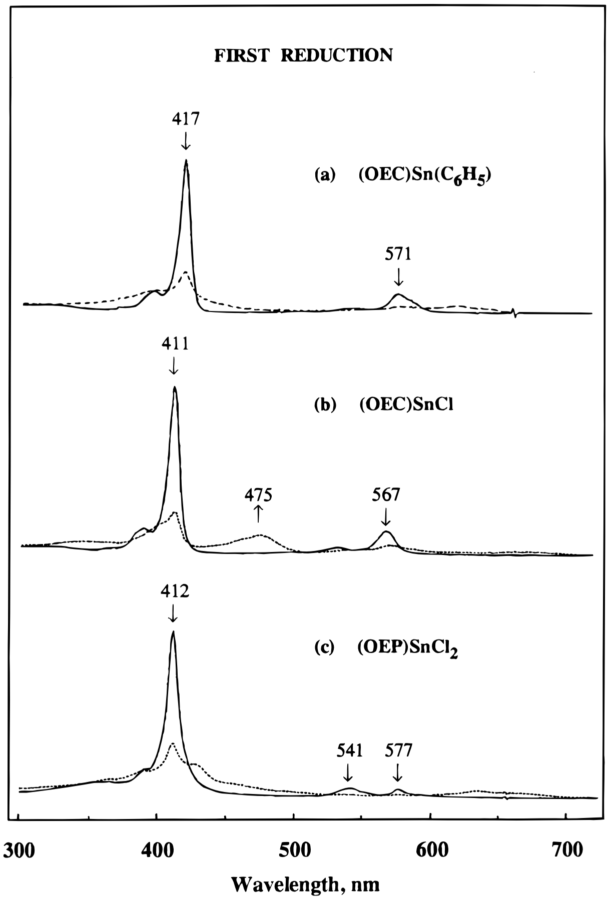

Figure 4. UV−visible spectral changes obtained during the first thin-layer controlled-potential reduction of (a) $(OEC)Sn(C_6H_5)$, (b) (OEC)-SnCl, and (c) $(OEP)SnCl_2$ in PhCN containing 0.2 M TBAP.

The spectrum of electroreduced (OEC)SnCl is different from that of electroreduced $(OEC)Sn(C_6H_5)$ or $(OEP)SnCl_2$ (see Figure 4). The most significant difference is a band at 475 nm for electroreduced (OEC)SnCl which is not observed for the other two compounds or for any other electroreduced Sn(IV) porphyrin.[14] However, a similar band is seen at around 480 nm for tin(II) porphyrins,[21,22] thus suggesting the formation of

---

(20) Molloy, K. C.; Purcell, T. G.; Quill, K.; Nowell, I. W. *J. Organomet. Chem.* **1984**, *267*, 237.

(21) Barbe, J.-M.; Ratti, C.; Richard, P.; Lecomte, C.; Gerardin, R.; Guilard, R. *Inorg. Chem.* **1990**, *29*, 4126.

a tin(II) corrole on the longer time scales needed for bulk controlled-potential reduction of (OEC)SnCl at −1.50 V. The conversion of a tin(IV) to a tin(II) corrole would require two electrons, and this was confirmed by thin-layer and bulk coulometry of (OEC)SnCl, which showed the addition of 1.6−1.8 electrons per molecule at an applied potential of −1.50 V. Thus, the coulometric and spectral data are self-consistent and suggest that the electroreduction of (OEC)SnCl involves an overall *two-electron* transfer to give a tin(II) product.

The cyclic voltammetric and coulometric data also suggest an electrochemical ECE-type mechanism in the first reduction of (OEC)SnCl,[23,24] with the products of the electrode reaction being reoxidized at $E_{pa} = -0.33$ and $+0.38$ V (see thin-layer voltammogram in Figure 3). A second reduction process is also seen for (OEC)SnCl at $E_{1/2} = -1.60$ V. This process has smaller peak currents than the first reduction (see Figures 2 and 3) and is assigned as due to an uncharacterized product of the chemical reaction following the first electron transfer step.

The electroreduction of (OEC)SnCl to give a Sn(II) product is "reversible" in that the coupled reoxidations at $E_{pa} = -0.33$ and $+0.38$ V both lead to species whose UV−visible spectra closely resemble the original tin(IV) corrole. The presence of two reoxidation peaks is then easily explained by the presence of two different counteranions, ClO_4^- and Cl^-, on the reoxidized species, i.e., by the generation of (OEC)SnCl at $E_{pa} = 0.38$ V and (OEC)SnClO$_4$ at $E_{pa} = -0.33$ V. This was confirmed by adding tetra-*n*-butylammonium chloride, TBACl, to solution. The peak of $E_{pa} = 0.38$ V increased and the peak of $E_{pa} = -0.33$ V decreased when TBACl was added.

Electrooxidation. (OEC)Sn(C_6H_5) and (OEC)SnCl undergo three reversible to quasireversible one-electron oxidations, in contrast to (OEP)SnCl_2, which undergoes only a single one-electron oxidation (see Figure 2 and Table 4). The three singly oxidized derivatives have similar UV−visible spectra with a decreased-intensity Soret band (see Figure 5), suggestive of a one-electron oxidized macrocycle.[26] The same singly oxidized $[(OEC)Sn(C_6H_5)]^+$ product could also be obtained by addition of 1 equiv of AgClO$_4$ to (OEC)Sn(C_6H_5) in PhCN. This species has an isotropic ESR signal centered at $g = 2.00$ and $\Delta H = 50$ or 24 G at 130 K or room temperature, respectively. This is also consistent with formation of a tin(IV) corrole π-cation radical.[27] Since metal-centered oxidations are not possible, the stepwise abstraction of two additional electrons from $[(OEC)Sn(C_6H_5)]^{+\bullet}$ and $[(OEC)SnCl]^{+\bullet}$ can only occur at the conjugated macrocycle leading to the formation of corrole dications and trications. The existence of a triply oxidized macrocycle thus distinguishes the corroles from the porphyrins and other related tetrapyrrole macrocycles, which undergo no more than two electrooxidations at the conjugated ring system with formation of π-cation radicals and dications.[8]

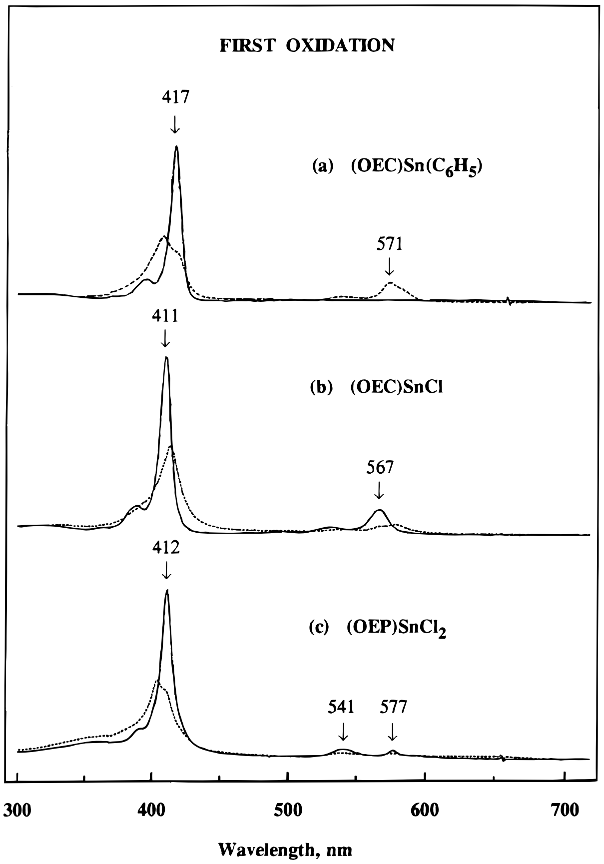

Figure 5. UV−visible spectral changes obtained during the first thin-layer controlled-potential oxidation of (a) (OEC)Sn(C_6H_5), (b) (OEC)SnCl, and (c) (OEP)SnCl_2 in PhCN containing 0.2 M TBAP.

Numerous examples exist in the porphyrin literature where reversible half-wave potentials for oxidation or reduction have been related to the site of electron transfer.[8] The most often utilized is the absolute potential difference between the first reversible oxidation and the first reversible reduction at the porphyrin macrocycle. This value, which is called the electrochemical HOMO−LUMO gap, is dependent upon the specific macrocycle and its substituents and is generally equal to 2.25 ± 0.15 V for "simple" octaethylporphyrin or tetraphenylporphyrin derivatives.[8] Surprisingly, the absolute potential difference between the first ring-centered oxidation and first ring-centered reduction of (OEC)Sn(C_6H_5) also ranges from 2.21 to 2.25 V depending on solvent (see Table 4), but further studies of other corroles with non-electroactive central metals are needed to ascertain if this HOMO−LUMO gap is general for the corroles or specific to the investigated compound. These studies are now in progress.

Acknowledgment. The support of the Robert A. Welch Foundation (K.M.K., Grant E-680) is gratefully acknowledged.

Supporting Information Available: Tables containing details of data acquisition and refinement, atomic coordinates and isotropic thermal parameters, bond lengths, bond angles, torsion angles, anisotropic thermal parameters and hydrogen coordinates, and isotropic displacement parameters (10 pages). Ordering information is given on any current masthead page.

IC980283K

---

(22) Kadish, K. M.; Dubois, D.; Barbe, J.-M.; Guilard, R. *Inorg. Chem.* **1991**, *30*, 4498.

(23) The cathodic peak potential for the first reduction of (OEC)SnCl shifts negatively by 37 ± 5 mV per 10-fold increase in scan rate, but there is no change in the "current function" $i_{pc}(I)/v^{1/2}$ or shape of the reduction peak ($|E_p - E_{p/2}| = 70$ mV), both of which are independent of scan rate. This suggests a coupled chemical reaction following an initial reversible to quasireversible one-electron transfer rather than a one-step two-electron Sn(IV)/Sn(II) reduction.[24] The actual mechanism would involve a fast one-electron reduction (observed in the "regular" cyclic voltammogram) followed by a chemical reaction (dissociation of the Cl^- counteranion) and addition of the second electron, i.e., an ECE electrochemical mechanism, probably of the type described in the literature for other tin(IV)/tin(II) reductions.[25]

(24) Nicholson, R. S.; Shain, I. *Anal. Chem.* **1964**, *36*, 706.

(25) Kadish, K. M.; Stamp, J.; Chemla, M.; Fatouros, N. *Anal. Lett.* **1973**, *6*, 909.

(26) See, for example: Felton, R. H. In *The Porphyrins*; Dolphin, D., Ed.; Academic Press: New York, 1978; Vol. 5, p 53 and references therein.

(27) Subramanian, J., In *Porphyrins and Metalloporphyrins*; Smith, K. M., Ed.; Elsevier: New York, 1975, p 555.